for a full three-dimensional boundary layer calculation with shock wave interaction. The development of such a complex computational model will require additional laser velocity measurements. These measurements should focus increased attention on the boundary layers and wakes. Data must be acquired on different fans at a variety of operating conditions.

## References


1 Dunker, R. J., Strinning, P. E., and Weyer, H. B., "Experimental Study of the Flow Field within a Transonic Axial Compressor Rotor by Laser Velocimetry and Comparison with Through-Flow Calculations," ASME Paper No. 77-GT-28, 1977.

2 Schodl, R., "Laser-Two-Focus Velocimetry (L2F) for Use in Aero Engines," *Laser Optical Measurements Methods for Aero Engine Research and Development*, Agard-LS-90, 1977.

3 Schodl, R., "Development of the Laser-Two-Focus Method for Non-Intrusive Measurement of Flow Vectors, Particularly in Turbomachines," ESA-TT-528, 1979.

4 Wisler, D. C., "Shock Wave and Flow Velocity Measurements in a High Speed Fan Rotor Using the Laser Velocimeter," ASME Paper No. 76-GT-49, ASME JOURNAL OF ENGINEERING FOR POWER, Apr 1977.

5 Weyer, H. B., "The Determination of Time-Weighted Average Pressures in Strongly Fluctuating Flows, Especially in Turbomachines," Technical Translation, ESRO-TT-161, 1974, p. 141.

6 McDonald, P. W., "The Computation of Transonic Flow Through Two-Dimensional Gas Turbine Cascades," ASME Paper No. 71-GT-89, 1971.

7 Epstein, A. H., Kerrebrock, J. L., and Thompkins, Jr., W. T., "Shock Structure in Transonic Compressor Rotors," *AIAA Journal*, Vol. 17, Apr 1979, pp. 375–379.


# Discussion

**D. C. Prince, Jr.**[1] In a recent paper (reference [8]), I proposed a pattern of characteristic features observed in experiments on a number of transonic compressor rotors. Table 1 is reproduced from reference [8], summarizing these features. I am gratified to see that the material covered in the present paper appears to be in general agreement with the material used in establishing that pattern and I hope that the authors may comment on their experience as it relates to this pattern.

The material in the paper provides evidence particularly relevant to items (1) and (3) of Table 1. Table 2 has been prepared from material in the present paper. Upstream vector angles given in the text were plotted in Figs. 10 and 14. Wave angles from the upstream vector to Mach number contours were measured with a protractor and used in the table. Recognizing the difficulty of obtaining reliable values from small scale figures, it is hoped that the authors can confirm these values or supply a more accurate replacement.

Figure 17 has been prepared using standard shock equations (e.g. reference [9], Chapter 10) and the data given for Fig. 10 ($M_{1R} = 1.307$, $\beta_1 = 24.04$) to assist in discussion of these items. Knowledge of the upstream Mach number and the wave angle provides enough information for a prediction of the discontinuity level to be expected. Applying Fig. 17 to the 55 deg wave angle upstream of the rotor for the measured data of Fig. 10 shows that the shock downstream Mach number is expected to be 1.19. Deceleration from Mach number 1.307 to Mach number 1.19 appears to require about double the pressure discontinuity shown on Fig. 10. The 53 deg wave angle upstream of the rotor in the calculated data of Fig. 10 calls for deceleration to Mach number 1.24, which is much more consistent with the discontinuity shown in the figure. It is surprising that both the calculated and the measured data should show larger upstream wave angles (54 and 56 deg) with wide open discharge than the 53 and 55 deg values at peak efficiency.

Inside the passage, the 62 deg wave angle for the measured data in Fig. 10 calls for deceleration from the upstream Mach number to 1.05. If the shock downstream Mach number is to be 1.15, as given in the text, the wave angle should have been 57 deg. The measured data in Fig. 14 for the region near the leading edge show deceleration from a Mach number above 1.38 to a Mach number slightly below 1.28 across a front nearly perpendicular to the flow, which is rather surprising in view of the data in Figure 17. For the calculated data of Fig. 10, the 61 deg wave angle calls for deceleration to Mach number 1.075, which is a substantially larger discontinuity than is shown on the figure. The calculated data in Fig. 14 show an oblique shock discontinuity extending about one-third of the way across the passage from the leading edge and then disappearing. It would be interesting to explore momentum and continuity balances for control volumes defined upstream of the discontinuity, along a selection of mid passage streamlines, back to the pressure surface along the Mach number 1.4 contour, and closed along the pressure surface.

In reference [8] I reported on the use of laser velocimeter (LV) data from reference [4] to infer the true wave angle. The fringe-type LV system had given direct measurements of momentum change components across the leading edge shock in axial and circumferential directions. The axial momentum was constant across the shock within a resolution of ±3 percent. If the axial momentum is constant, the wave orientation should be axial, so that the momentum change vector can be perpendicular to the wave. Analysis using the equations of Fig. 17 showed that a 5 deg inclination of the wave in either direction from the axial should correspond to 10 percent change in the axial momentum, so that the measurements defined a wave direction within 2 deg of axial. I hope that analysis of the L2F data for the present paper has included similar definition of the wave direction. Fig. 1 suggests that L2F measurements of the shock discontinuity were made for at least three axial positions along the 89 percent span stream surface. The data of Fig. 17 have been resolved into axial and circumferential components of the velocity discontinuity and presented as Fig. 18. From Fig. 18 one may infer that the axial velocity should have increased 3 percent to support the 62 deg wave angle from the measured data of Fig. 10. It is hoped that the authors will supply some detail on their measurements of the discontinuity, so that the wave angle and the uniformity of the shock strength can be confirmed.

[1] Consulting Engineer, General Electric Company, Aircraft Engine Group, Cincinnati, Ohio 45415.

**Table 1 Supersonic compressor shock structure features**

| | |
|---|---|
| 1 | Wave angles approximate maximum deflection. |
| 2 | Suction surface pressures near the leading edge are below 80 percent of upstream. |
| 3 | Shock discontinuities are substantially below expectation. |
| 4 | Pressure surface pressures in supersonic passages respond to back pressure. |
| 5 | Passage and downstream shocks disappear at supersonic pressure levels. |

**Table 2 Flow properties deduced from Figs. 10 and 14**

| | | Peak Efficiency | | Wide Open Discharge | |
|---|---|---|---|---|---|
| Upstream Mach number (from text) | | 1.307 | | 1.321 | |
| Mach angle | | 49.9 | | 49.2 | |
| Shock branch | | Upstream | In Passage | Upstream | In Passage |
| Shock wave angle | L2F measurement | 55 | 62 | 56 | 67(?) |
| | Time marching computations | 53 | 61 | 54 | 42(?) |

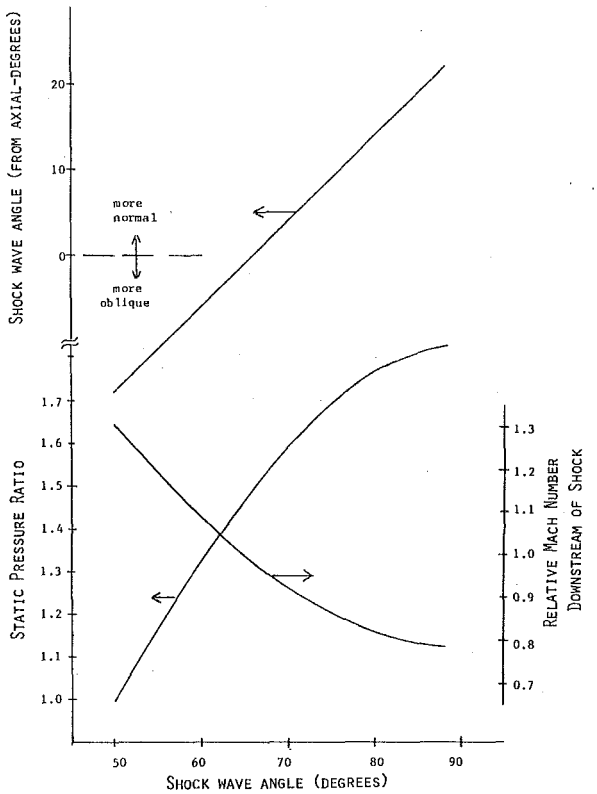


**Fig. 17 Predicted wave discontinuities—relative Mach number and static pressure ratio ($M_{1R}$ = 1.307; $\beta_1$ = 24.04 deg)**

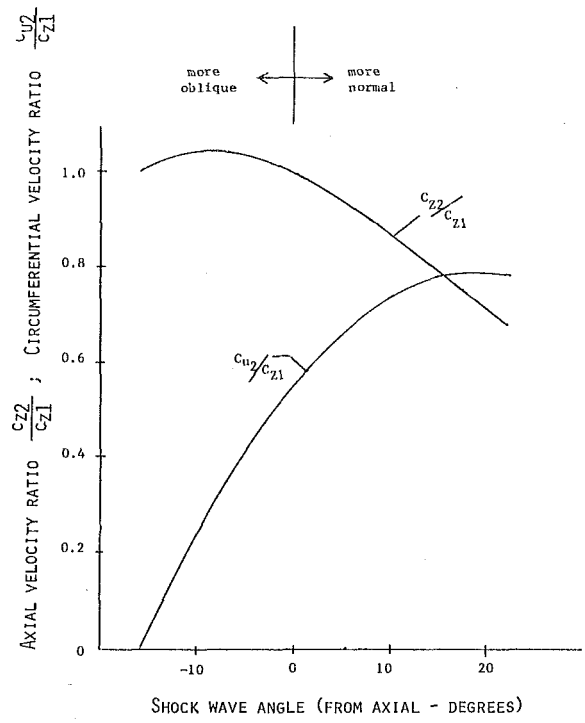


**Fig. 18 Predicted wave discontinuities—axial velocity ratio and circumferential velocity ratio ($M_{1R}$ = 1.307; $\beta_1$ = 24.04 deg)**

Experimental data included in the paper also seem to provide some support for items 4 and 5 of Table 1. I assume that Figs. 10 and 14 each show supersonic pressure surface velocity over the first 50 percent chord, which is presumably isolated from the downstream condition by the "Zone of Silence" concept. However, the Mach number at 25 percent chord on the pressure surface changes from 1.28 in Fig. 14 to about 1.08 in Fig. 10 as a result of throttling. Figure 14 shows a well-defined shock on the pressure surface at 50 percent chord, which has disappeared during throttling to Fig. 10. The experience behind reference [8] suggests that the static pressure rises across the rotor might be substantially less than those required for deceleration from Mach number 1.321 to Mach number 1.1 in Fig. 14, and from 1.307 to 0.9 in Fig. 10, so that this shock disappearance would have occurred at supersonic pressure levels. It would be helpful to know what total pressure loss distributions were used to infer the measured static pressures of Figs. 11, 13, and 15, and how these static pressures compare with measured profiles at rotor exit.

The experimental data in this paper could be used to formulate some requirements that should be met by a realistic blade-to-blade calculation procedure. According to my experience, the suction surface pressure near the rotor tip from the leading edge to the shock incidence does not vary with back pressure for Mach numbers higher than about 1.2. Pressure surface pressures, while remaining supersonic, may respond violently to back pressures. The large pressure surface variations in this paper have just been discussed. The suction surface pressures shown on Figs. 11, 13, and 15 seem indeed to be independent of the back pressure. However, integration of $dp/dr = \rho v^2/r$ along an orthogonal to the flow (taken, for example, at the midpoint of the cascade passage) should be consistent with the difference between the end point pressures. I suppose that these conditions can only be reproduced in a blade-to-blade calculation procedure if the lamina thickness distribution (streamtube thickness in the converging annulus) along the suction surface is independent of back pressure, while that along the pressure surface is a function of back pressure. Probably it is also important to make the strength of the shock discontinuity vary with back pressure. I interpret the text analysis as being restricted to laminae with circumferentially uniform thickness.

The pressure surface response to throttling should be expected, since the back pressure can be felt along the entire pressure surface at midspan, Fig. 8, where the passage flow is clearly subsonic. A rise in the midspan surface pressure should produce a tendency toward radial outflow along the pressure surface, leading to reduced effective lamina thickness near the rotor tip. This is not a viscous flow or secondary flow effect.

Reference [8] observed that obliquity of the passage shock in $S_2$ surfaces should have substantial influence on the passage shock strength. Figs. 7–10 show the passage shock to be incident on the suction surface at 22 percent chord at 18 percent span, 40 percent chord at 45 percent span, 50 percent chord at 68 percent span, and 70 percent chord at 89 percent span. Consequently, a substantial effect of $S_2$ surface obliquity might well be expected in this case also. Perhaps the authors would discuss how this effect is induced in their analysis, and in particular whether $S_2$ deflection across the passage shock has influenced the lamina thickness distribution which they use.

I wish to thank the authors again for publicizing so much useful information on supersonic/transonic rotor shock structure. Clearly, full explanations for all the features are not yet available. Sharing experiences should help to make progress.

### Additional References

8 Prince, D. C., Jr., "Three Dimensional Shock Structures for Transonic/Supersonic Compressor Rotors," AIAA Paper 79-0043, *AIAA Journal of Aircraft*, Jan. 1980, pp. 28–37.

9 Shapiro, A. H., *The Dynamics and Thermodynamics of Compressible Fluid Flow*, Ronald Press, New York, 1953.

## Authors Closure

The authors wish to thank Dr. Prince for his stimulating and thorough discussion. In general we agree with the observations and conclusions which he has presented. This closure will attempt to answer specific questions which have been raised in the discussion.

1 The interpretation of the magnitude of the wave angles given in the discussion appear to be accurate.

2 We have not devoted sufficient time to the evaluation of the measured or calculated wave angles to be able to explain discrepancies with simple theory. We assume that the differences which exist reflect

the inability of simple models to define a complex three-dimensional fan shock structure. Differences between the calculated and measured results also reflect the limitations of the present quasi three-dimensional model.

3 The increase in the upstream wave angle at the wide open discharge condition is primarily the result of a more negative leading edge suction surface incidence.

4 The total pressure loss used to infer the measured static pressures of Figs. 11, 13, and 15 were obtained from Mach number variations across the shock without considering the local wave angle.

5 We agree that the constraint of circumferentially constant streamtube thickness is undesirable but do not know the magnitude of its adverse effects.

6 The computed radial variation in shock position is influenced most strongly by the leading edge geometry and inlet air angle. The inlet air angle distribution along the span is influenced by the work input and blockage (both reflecting the shock strength) near the leading edge.